



Soft Matter

**Single Atoms and Small Clusters of Atoms May Accompany
Au and Pd Dendrimer-Encapsulated Nanoparticles**

Journal:	<i>Soft Matter</i>
Manuscript ID	SM-ART-04-2022-000518.R1
Article Type:	Paper
Date Submitted by the Author:	18-Jun-2022
Complete List of Authors:	Strasser, Juliette; The University of Texas at Austin Department of Chemistry, Chemistry Crooks, Richard; The University of Texas at Austin, Department of Chemistry

SCHOLARONE™
Manuscripts

[Prepared for publication as a Paper in *Soft Matter*]

Ms. ID:

**Single Atoms and Small Clusters of Atoms May Accompany Au and Pd
Dendrimer-Encapsulated Nanoparticles†**

Juliette W. Strasser and Richard M. Crooks*

Department of Chemistry and Texas Materials Institute, The
University of Texas at Austin, 2506 Speedway, Stop A5300,
Austin, TX 78712-1224, U.S.A.

*To whom correspondence should be addressed.

Email: crooks@cm.utexas.edu

†Electronic supplementary information (ESI) available. See DOI:

Submitted: 18 June, 2022

Abstract

We report the presence of small clusters of atoms (< 1 nm) (SCs) and single atoms (SAs) in solutions containing 1-2 nm dendrimer-encapsulated nanoparticles (DENs). Au and Pd DENs were imaged using aberration-corrected scanning transmission electron microscopy (ac-STEM), and energy dispersive spectroscopy (EDS) was used to identify and quantify the SAs/SCs. Two main findings have emerged from this work. First, the presence or absence of SAs/SCs depends on both the terminal functional group of the dendrimer ($-\text{NH}_2$ or $-\text{OH}$) and the elemental composition of the DENs (Au or Pd). Second, dialysis can be used to remove the majority of SAs/SCs in cases where a high density of SAs/SCs are present. The foregoing conclusions provide insights into the mechanisms for Au and Pd DEN synthesis and stability. Ultimately, these results demonstrate the need for careful characterization of systems containing nanoparticles to ensure that SAs/SCs, which may be below the detection limit of most analytical methods, are taken into consideration (especially for catalysis experiments).

Introduction

Nanoparticles (NPs) synthesized within and stabilized by a dendrimer template¹⁻³ are known as dendrimer-encapsulated nanoparticles (DENs). The resulting NPs are usually 1-2 nm in diameter and have typical size polydispersities of ± 0.2 nm.⁴⁻¹⁰ Because DENs are small and generally monodisperse, we^{5,11,12} and others¹³⁻¹⁵ have used them as model catalysts, with structure/function relationships that can be directly compared to first principles theory. The validity of the correlation between theory and experiment, however, relies upon a high level of confidence in the structure of the experimental model.

DENs have been extensively characterized using a variety of techniques, including electrochemical methods,^{4,5,16} UV-vis and NMR spectroscopy,¹⁷⁻¹⁹ X-ray absorption spectroscopy (XAS),^{7,20} and transmission electron microscopy (TEM).^{8,21} In recent years, the resolution of electron microscopy has greatly improved,²²⁻²⁴ and therefore we have taken the present opportunity to examine DENs at single-atom (SA) resolution using aberration-corrected scanning transmission electron microscopy (ac-STEM). The results show that in some cases the DEN synthesis is accompanied by the presence of SAs and small clusters (SCs) consisting of just a few atoms. This finding has important implications for using DENs as model catalysts.

ac-STEM is a powerful tool that allows for high-resolution NP characterization, and it is particularly useful for observing the presence of SAs/SCs in samples also containing NPs. For example, Petek et al. reported the presence of SAs in commonly used commercial NP catalysts.²⁵ Similarly, Duan et al. reported the unexpected presence of SAs/SCs alongside 3-5 nm RhAu NPs prepared using a microwave-assisted synthesis.²⁶ Finally, in another recent study, *in-situ* STEM was used to observe the generation of highly dynamic Pt SAs in Pt NP samples during CO oxidation.²⁷ Together, these representative studies highlight the importance of high-resolution ac-STEM imaging for thorough characterization of complex systems containing NPs, SAs, and SCs, especially when correlating catalyst structure to activity.

Here, we report the presence of SAs/SCs co-localized near 1-2 nm Au and Pd DENs. DEN samples were imaged via ac-STEM, and the identity and quantity of SAs/SCs were confirmed using energy dispersive spectroscopy (EDS). Notably, ac-STEM reveals SAs/SCs that have not been previously observed via XAS in similar DEN systems.^{4,20} There are two significant points about the DEN synthesis discussed in this report. First, the presence or absence of Au SAs/SCs are dependent on both the terminal functional group of the dendrimer ($-\text{NH}_2$ or $-\text{OH}$) and the elemental composition of the DENs (Au or Pd). Second, dialysis can be

used to remove the vast majority of SA/SCs in those cases where a high number density of SAs/SCs are present.

Experimental Section

Chemicals and materials. All chemicals were used as received unless otherwise noted. Sixth-generation poly(amidoamine) (PAMAM) dendrimers terminated with either amine groups (G6-NH₂) or hydroxyl groups (G6-OH) were purchased from Dendritech, Inc. (Midland, MI). Dendrimers were purchased as a 10-25% solution in methanol, which was removed under vacuum before use. Prior to synthesizing DENs, the dendrimers were resuspended in water at a concentration of 100 μ M. H₂AuCl₄·3H₂O (\geq 99.9%), K₂PdCl₄ (98%), NaBH₄ (99.99%), HCl (37% in H₂O), and a 1.0 M NaOH solution were purchased from MilliporeSigma (Burlington, MA). N₂ (99.9999%) and H₂ (99.999%) were purchased from Linde (Austin, TX).

Au DEN synthesis and dialysis. Dendrimers containing NPs having an average of 147 Au atoms (G6-NH₂(Au₁₄₇) and G6-OH(Au₁₄₇)) were synthesized in accordance with previously published literature reports.^{12,28} Briefly, 147 equiv. of a 20 mM H₂AuCl₄ solution were added dropwise to a stirred solution of 2.0 μ M G6-NH₂ or G6-OH dendrimer. After 2 min, an 11-fold excess of NaBH₄ was dissolved in a 0.30 M NaOH solution and then added to the stirred solution. The mixture was stirred for ~12 h in air at

22 ± 2 °C to deactivate excess BH_4^- . The final DEN concentration in solution was $2.0 \mu\text{M}$.

Note that the stoichiometry of the DENs (e.g., $\text{G6-NH}_2(\text{Au}_{147})$) represents the HAuCl_4 :dendrimer ratio used during synthesis, and consequently does not necessarily reflect a precise NP structure. We have, however, previously reported that this ratio controls the average diameter of DENs and that the size distribution is narrow (typically 0.2-0.3 nm).^{29,30} These comments also apply to the Pd DENs discussed next.

In some cases the $\text{G6-NH}_2(\text{Au}_{147})$ DEN solutions (pH ~12) were dialyzed against a 10.0 mM NaOH solution (pH 12) for 10-15 h using 12 kDa MWCO dialysis tubing (D6066, MilliporeSigma, Burlington, MA).¹² After removal from the first round of dialysis, the $\text{G6-NH}_2(\text{Au}_{147})$ DEN solutions were sometimes dialyzed for another 10-15 h under the same conditions. $\text{G6-OH}(\text{Au}_{147})$ DENs were not dialyzed.

Pd DEN synthesis and dialysis. The synthesis of $\text{G6-OH}(\text{Pd}_{147})$ DENs was also carried out according to previous literature procedures.^{18,31} Briefly, 147 equiv. of 20 mM K_2PdCl_4 were added dropwise to a stirred solution of $2.0 \mu\text{M}$ G6-OH dendrimer. This solution was stirred for 30 min under N_2 to yield a Pd-dendrimer complex, $\text{G6-OH}(\text{Pd}^{2+})_{147}$.¹⁸ Next, an 11-fold excess of NaBH_4 , dissolved in Milli-Q water, was added. This method resulted in a final $\text{G6-OH}(\text{Pd}_{147})$ concentration of $2.0 \mu\text{M}$.

The aforementioned procedure was modified for the synthesis of G6-NH₂(Pd₁₄₇) DENs.³¹ Synthesis of G6-NH₂(Pd₁₄₇) DENs requires adjustment of the solution pH to prevent crosslinking of primary amines by Pd²⁺ ions, which leads to aggregation and precipitation.³¹ In this case, 147 equiv. of 20 mM K₂PdCl₄ were added dropwise to a stirred solution of 2.0 μM G6-NH₂ dendrimer at pH 3. This solution was stirred for 30 min under N₂ to yield a Pd-dendrimer complex, G6-NH₂(Pd²⁺)₁₄₇.¹⁸ Next, a 40-fold excess of NaBH₄, dissolved in Milli-Q water, was added.³¹ A greater excess of NaBH₄ is required to reduce the G6-NH₂(Pd²⁺)₁₄₇ complex because of the lower initial solution pH. After reduction with NaBH₄, the solution pH was adjusted to ~7.5 using aqueous HCl.³¹ This method resulted in a final G6-NH₂(Pd₁₄₇) concentration of 2.0 μM.

For Pd DENs, the dialysis process was slightly different than the procedure described for Au DENs. To suppress oxidation of the Pd NPs, the G6-OH(Pd₁₄₇) DEN solutions (pH ~9) were dialyzed against a H₂-saturated, 0.01 mM NaOH solution (pH 9) for 10-15 h using 12 kDa MWCO dialysis tubing (D6066, MilliporeSigma, Burlington, MA).¹⁸ The dialysis was carried out in a H₂ environment inside a glove bag. Caution: H₂ gas is highly flammable when in contact with O₂. G6-NH₂(Pd₁₄₇) DENs were not dialyzed.

TEM and ac-STEM experiments. For imaging, continuous carbon-coated, 400 mesh Cu TEM grids were purchased from Electron Microscopy Sciences (Hatfield, PA). For EDS analysis, SiO₂-coated, 400 mesh Cu TEM grids were purchased from SPI Supplies (West Chester, PA). Samples were prepared by dropcasting 2.0 μ L of a 2.0 μ M DEN solution onto the TEM grid. Grids with Au DENs were dried in air and grids with Pd DENs were dried under N₂ in a glove bag.

Size analysis of Au and Pd DENs was carried out using a JEOL 2010f TEM with a point-to-point resolution of 0.19 nm and an accelerating voltage of 200 keV. For analysis of NP size, ImageJ was used to analyze 200 randomly selected NPs from three independently prepared samples. The data were subsequently fit using the Gaussian function in the OriginLab software package (Northampton, MA). EDS and ac-STEM were carried out using a JEOL Neoarm ac-STEM at an accelerating voltage of 80 keV and a resolution of 0.11 nm. EDS data were collected and analyzed using the Pathfinder software package from ThermoFisher Scientific.

Results and Discussion

Synthesis, qualitative characterization, and dialysis of Au

DENs. As discussed in the Experimental Section, PAMAM dendrimers were used to synthesize G6-NH₂(Au₁₄₇) and G6-OH(Au₁₄₇)

DENs. TEM analysis indicated that the diameter of the as-prepared DENs were 1.7 ± 0.2 nm and 1.6 ± 0.3 nm, respectively (**Figure S1**). These sizes are consistent with those reported previously.^{4,11,12,28}

Imaging via ac-STEM was carried out to characterize the G6-NH₂(Au₁₄₇) and G6-OH(Au₁₄₇) DENs. **Figure 1a** reveals the presence of two DENs, which are highlighted with white circles. In addition to these DENs, numerous small bright spots, corresponding to single atoms and small clusters of atoms (referred to hereafter as SAs/SCs), are also present. Qualitatively, the micrograph in **Figure 1a** suggests that the SAs/SCs are randomly and densely distributed. In addition to highlighting the location of the DENs, the white circles in **Figure 1a** represent the approximate size of the ~8 nm diameter dendrimers encapsulating the NPs.^{32,33} Importantly, there are a significant number of SAs/SCs beyond the perimeter of the circles. The origin of the SAs/SCs will be further addressed in a later section.

To determine whether the SAs/SCs can be removed, leaving behind just DENs, the G6-NH₂(Au₁₄₇) DENs were dialyzed. The dialysis was carried out for 10-15 h at pH 12, which matches the pH of the as-prepared DEN solution. TEM analysis indicated that dialysis does not change the size of the DENs (**Figure S2**). **Figure 1b** shows that after dialysis, the number of SAs/SCs

decreases substantially, and that the majority of the remaining SAs/SCs are located within the 8 nm circles that represent the dendrimers surrounding the NPs. This result suggests that following dialysis, the SAs/SCs are primarily localized within the interior cavity of the 6-9 nm-diameter dendrimer.³²⁻³⁴ This is in contrast to the pre-dialysis results (**Figure 1a**), which showed that SAs/SCs were randomly distributed over the TEM grid.

The G6-NH₂(Au₁₄₇) DEN solution was subject to a second round of dialysis using the same conditions as the first one. TEM analysis indicated that the second dialysis did not change the size of the DENs (**Figure S2**). Moreover, the SA/SC distribution was very similar to that resulting from the first dialysis (**Figure 1c**).

In addition to G6-NH₂(Au₁₄₇) DENs, we also characterized the SA/SC distribution alongside DENs synthesized using analogous hydroxyl-terminated dendrimers (G6-OH(Au₁₄₇), (**Figure 1d**)). Interestingly, there are far fewer SAs/SCs present in this case than for the undialyzed G6-NH₂(Au₁₄₇) DENs. This result implies that the SA/SC distribution in Au DENs depends on the terminal functional group at the periphery of the dendrimer (-NH₂ vs. -OH). This point will be discussed in more detail later.

To ensure that the observed SA/SCs are not composed of ionic forms of gold stabilized with ligands, such as Cl⁻, we carried out the following experiments. XPS spectra in the Au 4f

region were obtained for as-prepared and dialyzed G6-NH₂(Au₁₄₇) DENs, as well as for G6-OH(Au₁₄₇) DENs. The results, which are provided in **Figure S3**, indicate that there is no significant difference in the Au oxidation state of any of these DEN samples, despite the presence or absence of Au SAs/SCs.³⁵ Accordingly, we conclude that the SA/SCs are composed of zerovalent Au stabilized by dendrimers.

EDS quantification of SAs/SCs in Au DENs. To quantify the SA/SC distributions on TEM grids containing Au DENs, the Au EDS signal was collected in selected areas away from the edge of the dendrimers; that is, outside the white circles in (for example) **Figure 1**. More specifically, rather than counting individual SAs/SCs, which would be subject to size-dependent counting errors, we used the magnitudes of selected-area EDS signals as a proxy for the SA/SC density. Full details about how this procedure was implemented (**Section S1**) and the average values for the Au EDS signals (**Table S1**) are provided in the ESI. Briefly, however, the Au EDS signal was collected within a selected area, represented (for example) by the red box in **Figure 1a**. The Au EDS signal was subsequently normalized to a concurrently collected Si EDS signal, arising from the underlying SiO₂ coating on the Cu TEM grid, and then correlated to the presence of Au SAs/SCs. Control experiments demonstrating the reproducibility of EDS signals between

different areas of the same TEM grid, as well as between independently prepared TEM grids, are provided in **Figures S4-S6**.

Figure 2 compares the quantitative, normalized Au EDS signals for Au DENs. By far the highest Au EDS signals arise from the as-prepared G6-NH₂(Au₁₄₇) DENs. This result confirms that the bright spots in **Figure 1** are indeed Au SAs/SCs. Importantly, dialysis decreases the Au EDS signal by ~85%. A second round of dialysis does not, however, result in significant changes to the Au EDS signal, demonstrating that one round of dialysis is sufficient to remove the majority of SAs/SCs. To determine whether Au SAs/SCs resulted from incomplete reduction of the Au³⁺ precursor, G6-NH₂(Au₁₄₇) DENs were prepared using a 110-fold excess of NaBH₄ rather than the 11-fold excess used to obtain the data in **Figure 2**. Increasing the amount of NaBH₄ did not significantly change the Au EDS signal (**Figure S7**), and therefore we conclude that it is unlikely that the Au SAs/SCs arise from unreduced Au³⁺ ions carried over from synthesis.

The magnitude of the Au EDS signal for the as-prepared G6-OH(Au₁₄₇), hydroxyl-terminated DENs is also shown in **Figure 2**. In this case, the Au EDS signal is ~90% lower than the analogous signal for the as-prepared amine-terminated Au DENs. The difference in the Au EDS signal between the two types of as-prepared Au DENs indicates that changing the dendrimer terminal

group significantly affects the SA/SC distribution. This point will be discussed in more detail in the next section.

Finally, it is important to note that exposure to the electron beam does not significantly change the SA/SC distribution or EDS signal in the areas of the grid that were selected for analysis. Specifically, a selected area of the grid was continuously exposed to the electron beam for a 5 min period, and ac-STEM images were captured every 60 s during that period (**Figure S8**). EDS spectra were also collected in a selected grid area before and after a continuous 5 min beam exposure (**Figure S9**). The results of these experiments indicate that the majority of SAs/SCs in the region of interest are not generated from damage to NPs during electron beam exposure.

Mechanism of SA/SC stabilization in G6-NH₂(Au₁₄₇) DENs. On the basis of the experimental evidence discussed thus far, we conclude that SAs/SCs in G6-NH₂(Au₁₄₇) DEN solutions are stabilized by the primary amine groups at the periphery of the G6-NH₂ dendrimer. There are two main experimental results supporting this hypothesis. First, grids prepared with undialyzed G6-NH₂(Au₁₄₇) DEN solutions contain ~90% more SAs/SCs, as represented by the Au EDS signals in **Figure 2**, than the equivalent hydroxyl-terminated dendrimers. This experimental observation corresponds well to theoretical results reported by Camarada.^{36,37} Their findings showed that the terminal groups of

PAMAM dendrimers play a significant role in Au SC stabilization. Specifically, the terminal primary amines of the dendrimer were found to be the most stable coordination site for Au SCs containing between 2 and 8 atoms. In contrast, Au SC stabilization was found to be unfavorable at peripheral hydroxyl groups.

Second, as represented by the Au EDS signals in **Figure 2**, ~85% of SAs/SCs present in as-prepared G6-NH₂(Au₁₄₇) DEN solutions can be removed by dialysis. We propose that in undialyzed G6-NH₂(Au₁₄₇) DEN solutions, SAs/SCs are in equilibrium between the solution and the terminal amine groups of the dendrimer, with the equilibrium favoring complexation with the dendrimer. During dialysis, however, this equilibrium shifts toward the solution due to the large excess of dialysate. Consequently, ac-STEM and EDS analysis following dialysis reveal fewer SAs/SCs present in G6-NH₂(Au₁₄₇) DEN samples (**Figure 2**). Additionally, we propose that the equilibrium between the dendrimer and the solution is responsible for the high, uniform density of SAs/SCs on grids containing undialyzed G6-NH₂(Au₁₄₇) DENs. During drying, the weakly bound Au SAs/SCs in equilibrium between the dendrimer and solution are transported away from the dendrimer periphery and onto the grid surface.

To confirm that the SA/SCs are associated with the dendrimers and do not form in solution independent of the

dendrimers, we conducted the following control experiment. Specifically, the same synthesis used to prepare DENs was carried out, but in the absence of dendrimers. Under these conditions, a black precipitate formed upon reduction with NaBH_4 . After stirring the solution for ~12 h, 2 μL of the supernatant was dropcast onto a SiO_2 -coated 400 mesh Cu TEM grid for EDS analysis. In this case, no Au EDS signal above the background level of the TEM grid was detected. This result demonstrates that Au SAs/SCs do not form in solution, but rather requires stabilization by dendrimers.

Synthesis, characterization, and dialysis of Pd DENs. To better understand the ac-STEM and EDS results for Au DENs, Pd DENs were synthesized to probe the SA/SC distributions in these materials. Pd DENs were selected for this study because Pd^{2+} precursor ions have been shown to coordinate strongly and stoichiometrically to the interior tertiary amines of the dendrimer during DEN synthesis.^{17,31} In contrast, direct coordination to the interior of the dendrimer has not been observed for Au^{3+} ions.³⁰ Accordingly, we hypothesized that the SA/SC distribution would change based on how the metal precursor ions interact with the dendrimer. We also hypothesized that if SAs/SCs are present and stabilized by the interior tertiary amines of the dendrimer, rather than at the periphery of the

dendrimer, then the SA/SC distribution would not be dependent on the terminal functional group of the dendrimer.¹⁸

The method for synthesizing G6-OH(Pd₁₄₇) and G6-NH₂(Pd₁₄₇) DENs,^{18,31} which is somewhat different from the Au DEN synthesis, is provided in the Experimental Section. TEM analysis of the as-prepared G6-OH(Pd₁₄₇) DENs and G6-NH₂(Pd₁₄₇) DENs indicates their diameters to be 1.4 ± 0.2 nm and 1.5 ± 0.3 nm (**Figure S10**), respectively. These diameters are consistent with earlier reports.^{18,31}

After synthesis, the pH of the G6-OH(Pd₁₄₇) DEN solution was ~9. Moreover, Pd DENs must be kept in a H₂ environment to suppress oxidation of NPs back to the Pd²⁺-dendrimer complex.¹⁸ Therefore, dialysis of the G6-OH(Pd₁₄₇) DENs was carried out using a H₂-saturated pH 9 solution. Dialysis did not result in a size change of the DENs (**Figure S10**). The G6-NH₂(Pd₁₄₇) DENs were not dialyzed.

Imaging via ac-STEM was carried out to characterize Pd DENs (**Figure 3**). Because Pd is a lower-*Z* element than Au, and because ac-STEM is based on electron scattering, the contrast between the Pd atoms and the background is not as sharp as it is for Au. Nevertheless, the micrograph in **Figure 3a** shows that there are a relatively low number of Pd SAs/SCs present in the G6-OH(Pd₁₄₇) DEN sample, particularly compared to the G6-NH₂(Au₁₄₇) DEN sample (**Figure 1a**). Moreover, the SAs/SCs that are present

appear to be randomly distributed throughout the micrograph. Likewise, the micrograph in **Figure 3b** reveals that very few SAs/SCs are present in the G6-OH(Pd₁₄₇) DEN samples following dialysis. The micrograph of the G6-NH₂(Pd₁₄₇) DEN sample in **Figure 3c** exhibits a similar SA/SC distribution to the G6-OH(Pd₁₄₇) DEN sample in **Figure 3a**. These results suggest that, unlike for Au SAs/SCs, the Pd SA/SC distribution is not dependent on the terminal functional group of the dendrimer.

As for the Au DENs, the SA/SC distribution for grids prepared with Pd DENs was quantified using EDS. Care was taken to only analyze regions of the grids away from the NPs. The average values for the Pd EDS signals are provided in **Table S2**, and **Figure 4** compares the normalized Pd EDS signals for the Pd DENs. Importantly, there is no significant difference between the Pd EDS signals for grids prepared with G6-OH(Pd₁₄₇) and G6-NH₂(Pd₁₄₇) DENs. This result confirms that the Pd SA/SC distribution is not affected by the terminal functional group of the dendrimer. Additionally, there is no significant change to the Pd EDS signal for grids prepared using G6-OH(Pd₁₄₇) DENs following one round of dialysis, showing that Pd SAs/SCs are stable during dialysis. We conclude that there are very few Pd SAs/SCs present on grids prepared using Pd DENs, and the SAs/SCs that are present are likely not stabilized by the terminal amine or hydroxyl groups of the dendrimer.^{17,31} Significantly, this

result represents a fundamental difference between the mechanism of SA/SC formation and stabilization in Au and Pd DENs.

Summary and Conclusions

We used ac-STEM and EDS to identify, characterize, and quantify SAs/SCs in solutions containing Au and Pd DENs. There are two important conclusions that arise from this study. First, the presence or absence of SAs/SCs are dependent on both the terminal functional group of the dendrimer ($-\text{NH}_2$ or $-\text{OH}$) and the elemental composition of the DENs (Au or Pd). Second, dialysis can be used to remove the majority of SAs/SCs in cases where a high density of SAs/SCs are present. We conclude that, when present, Au SAs/SCs are stabilized by an equilibrium between the amine group of the dendrimer and the solution. Together, these findings provide insight into Au and Pd DEN synthesis and stabilization and demonstrate a method to remove the majority of Au SAs/SCs from Au DENs.

The results discussed here may have significant implications for catalysis using DENs, as recent studies have shown that ensembles containing NPs and SAs/SCs can have different catalytic properties than NPs alone.^{38,39} Additionally, SAs/SCs have been predicted, and recently observed, to be dynamic contributors to catalytic processes.^{27,40} Consequently, thorough characterization of DEN systems, which may contain NPs

and SAs/SCs, is essential, particularly when using DENs as a model system for comparing theory to experiment.⁴¹ Experiments using Au DENs to probe the effect of SAs/SCs on catalytic activity are underway and will be reported in due course.

Author Contributions

J.W.S. was responsible for experimental design, data collection and analysis, initial manuscript preparation, and manuscript editing. R.M.C. was responsible for experimental design, project administration, funding acquisition, and manuscript editing and review. Both authors have read and agreed to the published version of this manuscript.

Conflicts of Interest

The authors declare no conflict of interest.

Acknowledgements

We gratefully acknowledge support from the Chemical Sciences, Geosciences, and Biosciences Division, Office of Basic Energy Sciences, Office of Science, U.S. Department of Energy (Contract: DE-SC0010576). We thank the Robert A. Welch Foundation (Grant F-0032) for sustained support of our research. J.W.S. acknowledges support from the Provost's Graduate Excellence Fellowship. We thank Dr. Jonathan R. Thompson (UT

Austin) for helpful discussions. We also thank Ms. Aigerim Galyamova (UT-Austin) for her assistance with XPS data collection and analysis.

References

- 1 D. A. Tomalia and J. M. J. Fréchet, *J. Polym. Sci. Part A Polym. Chem.*, 2002, **40**, 2719–2728.
- 2 D. A. Tomalia, H. Baker, J. Dewald, M. Hall, G. Kallos, S. Martin, J. Roeck, J. Ryder and P. Smith, *Polym. J.*, 1985, **17**, 117–132.
- 3 P. K. Maiti, T. Çağın, S. T. Lin and W. A. Goddard, *Macromolecules*, 2005, **38**, 979–991.
- 4 J. W. Strasser, T. J. P. Hersbach, J. Liu, A. S. Lapp, A. I. Frenkel and R. M. Crooks, *ChemElectroChem*, 2021, **8**, 2545–2555.
- 5 J. A. Trindell, Z. Duan, G. Henkelman and R. M. Crooks, *ChemElectroChem*, 2020, **7**, 3824–3831.
- 6 K. Yamamoto, T. Imaoka, M. Tanabe and T. Kambe, *Chem. Rev.*, 2019, **120**, 1397–1437.
- 7 R. Ye, A. V Zhukhovitskiy, R. V Kazantsev, S. C. Fakra, B. B. Wickemeyer, F. Dean Toste and G. A. Somorjai, *J. Am. Chem. Soc.*, 2018, **140**, 4144–4149.
- 8 Y. Ju, H.-J. Ro, Y. Yi, T. Cho, S. Il Kim, C. W. Yoon, S. Jun and J. Kim, *Anal. Chem.*, 2021, **93**, 2871–2878.
- 9 A. Galyamova and R. M. Crooks, *Nanomaterials*, 2022, **12**, 855.
- 10 N. C. Antonels, M. Benjamin Williams, R. Meijboom and M. Haumann, *J. Mol. Catal. A Chem.*, 2016, **421**, 156–160.
- 11 A. Galyamova, K. Shin, G. Henkelman and R. M. Crooks, *J.*

- Phys. Chem. C*, 2020, **124**, 10045–10056.
- 12 A. S. Lapp, Z. Duan, N. Marcella, L. Luo, A. Genc, J. Ringnalda, A. I. Frenkel, G. Henkelman and R. M. Crooks, *J. Am. Chem. Soc.*, 2018, **140**, 6249–6259.
- 13 Z. D. Pozun, S. E. Rodenbusch, E. Keller, K. Tran, W. Tang, K. J. Stevenson and G. Henkelman, *J. Phys. Chem. C*, 2013, **117**, 7598–7604.
- 14 X. Yan, Y. Luo, W. Liu, L. Liang, Y. Gan, Z. Chen, Z. Xu, H. Wan, D. Tang, H. Shi and J. Hu, *Phys. Chem. Chem. Phys.*, 2020, **22**, 6222–6230.
- 15 M. Welborn, W. Tang, J. Ryu, V. Petkov and G. Henkelman, *J. Chem. Phys.*, 2011, **135**, 014503.
- 16 K. Yamamoto, T. Imaoka, W. J. Chun, O. Enoki, H. Katoh, M. Takenaga and A. Sonoi, *Nat. Chem.*, 2009, **1**, 397–402.
- 17 M. V. Gomez, J. Guerra, A. H. Velders and R. M. Crooks, *J. Am. Chem. Soc.*, 2009, **131**, 341–350.
- 18 E. V Carino, M. R. Knecht and R. M. Crooks, *Langmuir*, 2009, **25**, 10279–10284.
- 19 D. Yamamoto, S. Watanabe and M. T. Miyahara, *Langmuir*, 2010, **26**, 2339–2345.
- 20 Z. Duan, Y. Li, J. Timoshenko, S. T. Chill, R. M. Anderson, D. F. Yancey, A. I. Frenkel, R. M. Crooks and G. Henkelman, *Catal. Sci. Technol.*, 2016, **6**, 6879.
- 21 Y. Borodko, P. Ercius, V. Pushkarev, C. Thompson and G.

- Somorjai, *J. Phys. Chem. Lett*, 2012, **3**, 236–241.
- 22 S. J. Pennycook, *Ultramicroscopy*, 2012, **123**, 28–37.
- 23 O. L. Krivanek, T. C. Lovejoy and N. Dellby, *J. Microsc.*, 2015, **259**, 165–172.
- 24 P. Tieu, X. Yan, M. Xu, P. Christopher and X. Pan, *Small*, 2021, **17**, 2006482.
- 25 U. Petek, F. Ruiz-Zepeda, M. Bele and M. Gaberšček, *Catalysts*, 2019, **9**, 134–145.
- 26 Z. Duan, J. Timoshenko, P. Kunal, S. D. House, H. Wan, K. Jarvis, C. Bonifacio, J. C. Yang, R. M. Crooks, A. I. Frenkel, S. M. Humphrey and G. Henkelman, *Nanoscale*, 2018, **10**, 22520–22532.
- 27 L. Liu, D. N. Zakharov, R. Arenal, P. Concepcion, E. A. Stach and A. Corma, *Nat. Commun.*, 2018, **9**, 574.
- 28 J. A. Trindell, J. Clausmeyer and R. M. Crooks, *J. Am. Chem. Soc.*, 2017, **139**, 16161–16167.
- 29 V. S. Myers, M. G. Weir, E. V Carino, D. F. Yancey, S. Pande and R. M. Crooks, *Chem. Sci.*, 2011, **2**, 1632–1646.
- 30 Y.-G. Kim, S.-K. Oh and R. M. Crooks, *Chem. Mater.*, 2004, **16**, 167–172.
- 31 R. W. J. Scott, H. Ye, R. R. Henriquez and R. M. Crooks, *Chem. Mater.*, 2003, **15**, 3873–3878.
- 32 V. V Tsukruk, F. Rinderspacher and V. N. Bliznyuk, *Langmuir*, 1997, **13**, 2171–2176.

- 33 A. Hierlemann, J. K. Campbell, L. A. Baker, R. M. Crooks and A. J. Ricco, *J. Am. Chem. Soc.*, 1998, **120**, 5323–5324.
- 34 M. Gosika and P. K. Maiti, *Soft Matter*, 2018, **14**, 1925–1938.
- 35 NIST X-ray Photoelectron Spectroscopy (XPS) Database, Version 4.1, <https://srdata.nist.gov/xps/Default.aspx>, (accessed 16 June 2022).
- 36 M. B. Camarada, *J. Phys. Chem. A*, 2017, **121**, 8124–8135.
- 37 M. B. Camarada, *Chem. Phys. Lett.*, 2016, **654**, 29–36.
- 38 C. Rivera-Cárcamo, I. C. Gerber, I. del Rosal, B. Guicheret, R. Castro Contreras, L. Vanoye, A. Favre-Réguillon, B. F. Machado, J. Audevard, C. de Bellefon, R. Philippe and P. Serp, *Catal. Sci. Technol*, 2021, **11**, 984–999.
- 39 P. Serp, *Nanoscale*, 2021, **13**, 5985–6004.
- 40 L. Liu, D. M. Meira, R. Arenal, P. Concepcion, A. V. Puga and A. Corma, *ACS Catal.*, 2019, **9**, 10626–10639.
- 41 J. A. Trindell, Z. Duan, G. Henkelman and R. M. Crooks, *Chem. Rev.*, 2020, **120**, 814–850.

Figure Captions

Figure 1. ac-STEM images of (a) as-prepared G6-NH₂(Au₁₄₇) DENs, (b) once-dialyzed G6-NH₂(Au₁₄₇) DENs, (c) twice-dialyzed G6-NH₂(Au₁₄₇) DENs, and (d) as-prepared G6-OH(Au₁₄₇) DENs. The white circles in (a) and (b) represent the approximate locations of the 6–9 nm dendrimers encapsulating the NPs. The red box in (a) denotes a representative area used to collect EDS spectra. TEM grids for ac-STEM analysis were prepared by dropcasting 2 μ L of Au DEN solution onto a continuous carbon-coated, 400 mesh Cu TEM grid and drying in air. The scale bar is 5 nm.

Figure 2. Histograms showing Au EDS signals collected in areas of a grid in which DENs were not present (such as the one represented by the red box in **Figure 1a**). The Au EDS signals were normalized to the Si EDS signal arising from the underlying SiO₂ coating on the TEM grids (see the ESI). The error bars represent the standard deviation from the mean for Au EDS signals obtained from 10 EDS spectra collected within one grid square. TEM grids for EDS analysis were prepared by dropcasting 2 μ L of Au DEN solution onto a SiO₂-coated, 400 mesh Cu TEM grid and drying in air.

Figure 3. ac-STEM images of (a) as-prepared G6-OH(Pd₁₄₇) DENs, (b) dialyzed G6-OH(Pd₁₄₇) DENs, and (c) as-prepared G6-NH₂(Pd₁₄₇)

DENs. TEM grids for ac-STEM analysis were prepared by dropcasting 2 μL of Pd DEN solution onto a continuous carbon-coated, 400 mesh Cu TEM grid and drying under N_2 . The scale bar is 5 nm.

Figure 4. Histograms showing the Pd EDS signal collected in areas of a grid in which DENs were not present. The Pd EDS signals were normalized to the Si EDS signal arising from the underlying SiO_2 coating of the TEM grid (see the ESI). The error bars represent the standard deviation from the mean for Pd EDS signals obtained from 10 EDS spectra collected within one grid square. TEM grids for EDS analysis were prepared by dropcasting 2 μL of Pd DEN solution onto a SiO_2 -coated, 400 mesh Cu TEM grid and drying under N_2 .

Figures

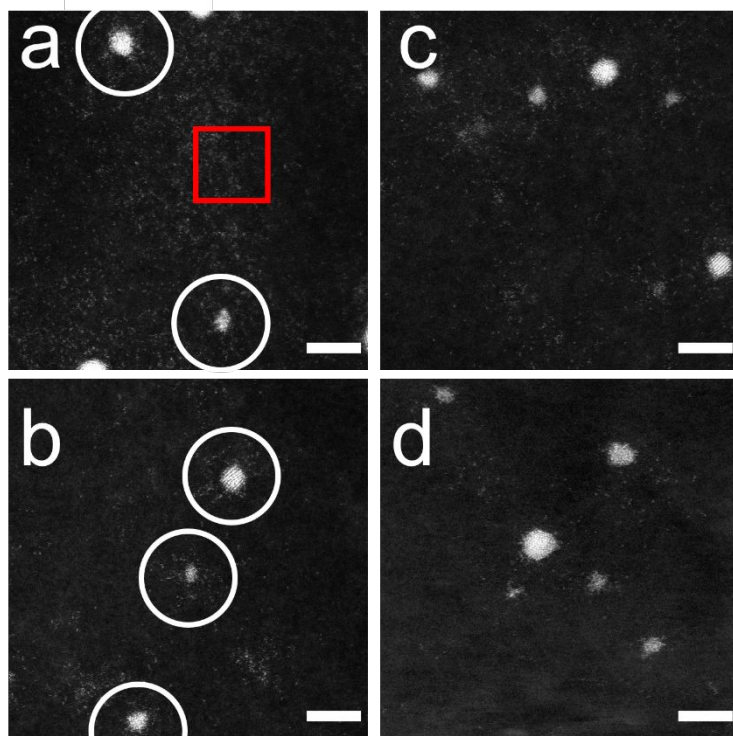


Figure 1 / Strasser and Crooks

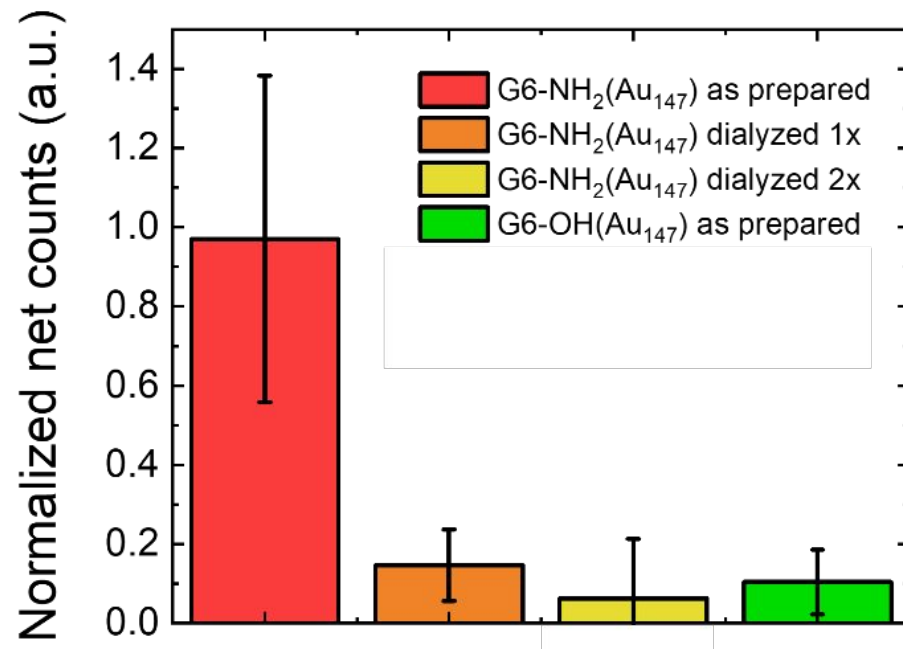


Figure 2 / Strasser and Crooks

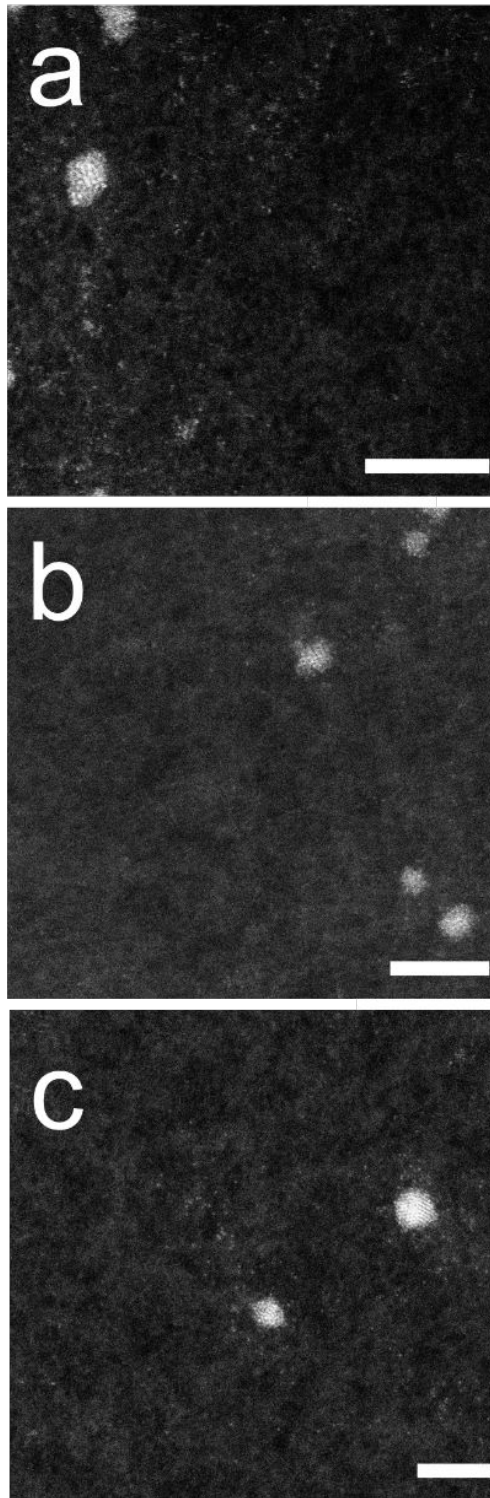


Figure 3 / Strasser and Crooks

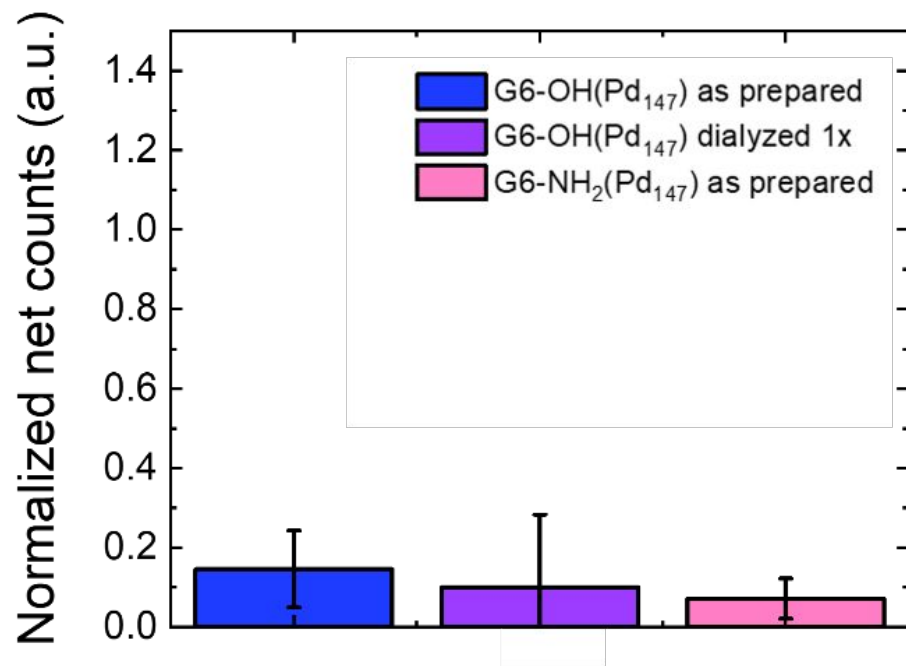


Figure 4 / Strasser and Crooks